Journal of Biotechnology 359 (2022) 75–81

Contents lists available at ScienceDirect

Journal of Biotechnology

journal homepage: www.elsevier.com/locate/jbiotec

P3HT-based organic field effect transistor for low-cost, label-free detection of immunoglobulin G

Hao Runfang [a,b], Yue Yangfan [a,b], Li Leilei [a,b], Ji Jianlong [a,b], Zhang Qiang [a,b], Ding Lifeng [c], Sang Shengbo [a,b], Li Qiang [a,b,*]

[a] Shanxi Key Laboratory of Micro Nano Sensors & Artificial Intelligence Perception, College of Information and Computer, Taiyuan University of Technology, Taiyuan 030024, China
[b] Key Lab of Advanced Transducers and Intelligent Control System of the Ministry of Education, Taiyuan University of Technology, Taiyuan 030024, China
[c] Department of Chemistry and Chemical Engineering, Taiyuan Institute of Technology, Taiyuan 030008, China

ARTICLE INFO

Keywords:
Poly(3-hexylthiophene)
Organic field effect transistor
Immunoglobulin G

ABSTRACT

Currently, organic field effect transistors (OFETs) are widely used in the field of biodetection because of their inherent gain amplification function and good biocompatibility. However, the vast majority of OFET biosensors have disadvantages including a long preparation cycle, complicated processing and expensive materials. Thus, this paper proposes a simple and inexpensive preparation method for label-free detection of immunoglobulin G (IgG). In this work an active dielectric bilayer field effect transistor with 3D-printed silver source and drain electrodes was used. The active layer was modified by physically adsorbing an anti-IgG antibody on P3HT as a recognition element and then sealed with bovine serum albumin (BSA) to prevent nonspecific adsorption. The carrier mobility of the bilayer dielectric layer active field effect transistor reached 4.6 × 10^{-2} cm^2/Vs, and the dynamic detection range for IgG spanned 6 orders of magnitude with a detection limit of 2.9 Picomolar (pM). Controlled experiments demonstrated that the developed sensor has high selectivity for IgG. Overall, this easy-to-operate and low-cost OFET biosensor has broad commercialization prospects and lays the foundation for the early clinical detection of disease-causing biomolecules.

1. Introduction

Immunoglobulin is secreted by plasma cells for defence against pathogens when the body's immune system is attacked. According to the amino acid sequence and arrangement structure of immunoglobulins, they can be divided into IgA, IgG, IgM, IgD and IgE (Di and Yaofeng, 2021), of which IgG is the most abundant in serum, accounting for approximately 75 % of the total immunoglobulins. The immunity of the human body is largely dependent on IgG content. When the concentration of IgG is too high, immune disorders may occur, leading to immune diseases such as systemic lupus erythematosus (Jian, 2021; Qian and Bin, 2021; Shikun, 2022). However, a low IgG concentration can lead to low immunity of the body and cause infectious diseases (Lanxia, 2018; Jiajun et al., 2020). Thus, there is an urgent need for a sensor with high sensitivity, high selectivity and a wide detection range for IgG serum content for the early prevention and monitoring of immune diseases.

A number of methods have been used for IgG detection, including radioimmunoassays (RIAs), enzyme-linked immunosorbent assays (ELISAs), and fluorescent immunoassays (Spindel et al., 2015; Kikuti et al., 2018; Pas et al., 2013; Santos et al., 2012; Frisk et al., 1984). However, these methods require the labelling of specific target analytes, which is cumbersome and time-consuming. To achieve label-free detection of biomolecules, researchers have developed quartz crystal microbalance (QCM) and surface plasmon resonance (SPR) biosensors (Janmanee et al., 2011; Zhou et al., 2021; Wu et al., 2016; Mizutani et al., 2012). These methods are still cumbersome to operate and use expensive instruments and materials, making the low-cost commercial preparation of sensors difficult. OFETs can achieve conversion of small biological signals to larger electrical signals due to their inherent gain amplification function, suggesting that OFET-based sensors may have promising applications in biomolecular detection (Lin and Yan, 2012; Syu et al., 2018; Wang et al., 2019).

OFETs exhibit high sensitivity, enabling the conversion and

* Corresponding author at: Shanxi Key Laboratory of Micro Nano Sensors & Artificial Intelligence Perception, College of Information and Computer, Taiyuan University of Technology, Taiyuan 030024, China.
E-mail address: liqiang02@tyut.edu.cn (L. Qiang).

https://doi.org/10.1016/j.jbiotec.2022.09.022
Received 3 July 2022; Received in revised form 12 September 2022; Accepted 28 September 2022
Available online 3 October 2022

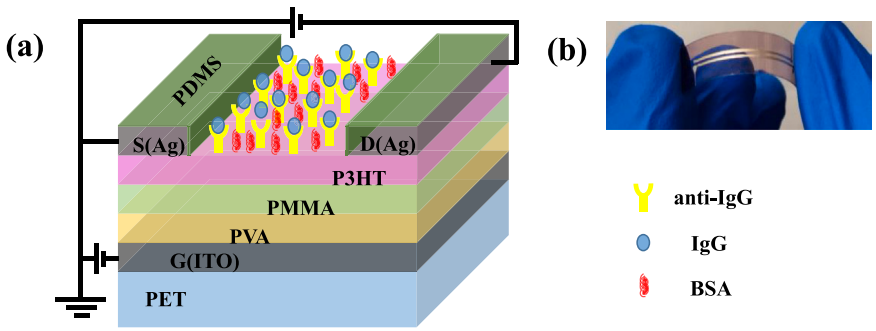

Fig. 1. (a) Schematic diagram of bottom gate top contact structure P3HT OFET for label-free detection of IgG and (b) picture of the bent sensor.

amplification of biological signals. In addition, the specific binding of the recognition element to the corresponding target analyte allows for highly selective detection. The recognition element can modify the electrode, the dielectric layer and the active layer (Wang et al., 2019), and the binding of the immobilized recognition element to the target biomolecule changes the charge distribution in the channel, causing a change in the relevant parameters of the transistor, thus enabling the detection of biomolecules. Stefano Casalini et al. detected dopamine in vitro through gate modification by a self-assembled monomolecular layer (SAM) of cysteamine (CA) and 4-formylphenylboronic acid (BA) (Casalini et al., 2013). Eleonora Macchia et al. used a chemical SAM (chem-SAM)-functionalized gate to achieve C-reactive protein (CRP) detection through specific binding of an antigen and antibody (MacChia et al., 2019). Sunil Kumar Sailapu et al. developed a self-powered platform for HIV-specific detection using a chem-SAM functionalized gate and a built-in paper-based biofuel cell (BFC) (Sailapu et al., 2020). Maria Magliulo et al. modified the dielectric layer by spin-coating streptavidin (SA), allowing P3HT and SA to form a functional biological interlayer (FBI) for biotin detection (Magliulo et al., 2013). Mallory L. Hammock et al. modified gold nanoparticles using chloroauric acid reduction on the active layer to immobilize the recognition element by Au-S bonding, enabling the detection of thrombin (Hammock et al., 2013). However, the above immobilization methods chemically modified or disrupted the conformation of the functionalized layer (functionalized channel, functionalized electrolyte and functionalized gate), which had impacted the performance of the transistor before detecting the target biomolecule (Albers et al., 2012; Awsiuk et al., 2014; Awsiuk et al., 2016). Therefore, to maintain transistor performance, the intermolecular forces between the functionalized layer and the biomolecule need to immobilize the recognition element. Physical adsorption is a commonly used method that is not only simple and fast but also does not involve chemical bonding between the biomolecule and the functionalized layer, immobilizing the biomolecule only through weak interactions such as hydrophobic interactions and van der Waals forces (Lin and Yan, 2012). The physical adsorption of recognition elements on the active layer has been reported for the detection of target biomolecules. Magliulo et al. (2016) achieved a highly sensitive, label-free detection of CRP by physisorption of anti-CRP on the P3HT active layer. Seshadri et al. (2018) developed an electrolyte-gated OFET for label-free detection of procalcitonin with detection limits as low as pM by physisorption of anti-PCT on the P3HT layer. However, the complex electrode deposition process, often involving photolithography (Kim et al., 2020), electron beam evaporation (Vasilyeva et al., 2018; Huynh et al., 2019; Sun et al., 2015), magnetron sputtering (Cao et al., 2019; Shi et al., 2020; Ferhati et al., 2019), etc., and the high cost of electrode materials hinder their commercial application.

To this end, a low-cost, label-free P3HT OFET biosensor was developed for IgG detection. A silver-sourced drain electrode was prepared using 3D printing because silver is not only inexpensive but also matches the highest occupied molecular orbital (HOMO) of P3HT in terms of its work function (about 5.1 eV) after high-temperature annealing, facilitating carrier injection (Xue et al., 2005). In addition, the higher carrier mobility of the OFET with a double dielectric layer allows for highly sensitive detection of IgG. Finally, anti-IgG is physically adsorbed directly on the P3HT active layer as a recognition element for capturing IgG, and then BSA is used as an adsorption blocker to avoid nonspecific adsorption without any additional processing required to modify or change the chemical bond between the active layer and the biomolecule, maintaining biomolecular integrity and eliminating the need for labelling. Notably, the designed P3HT OFET biosensor has a high electrical performance (carrier mobility of approximately 10^{-2} cm2/Vs) and a wide dynamic detection range (spanning 6 orders of magnitude) with a detection limit of 2.9 pM.

2. Experimental section

2.1. Reagents

Conductive silver paste was purchased from DuPont, USA. Regionally regularized poly(3-hexylthiophene) RR-P3HT (regularity >98 %, molecular weight 50 kDa) was purchased from Sigma—Aldrich and did not require further purification as an active layer channel. Polyvinyl alcohol (PVA, molecular weight 130 kDa), polymethyl methacrylate (PMMA, molecular weight 120 kDa), anisole (AR, 99 %) and o-dichlorobenzene (AR, 99 %) were purchased from Shanghai Maclean Biochemical Technology Co. Polyethylene terephthalate (PET) film (thickness 0.125 mm) and ITO film (transmittance 83 %) were purchased from Shenzhen Rigorous Technology Co. Rabbit IgG, horseradish peroxidase-labelled sheep anti-rabbit IgG polyclonal antibody (anti-IgG molecular weight 150 kDa), bovine serum protein (BSA, molecular weight 66 kDa) and phosphate buffer (PBS) were purchased from Shanghai Haling Biotechnology Co. Carcinoembryonic antigen (CEA, molecular weight 965.08 kDa) were purchased from Beijing Dehang Wuzhou Technology Co. Human serum albumin (HSA, specification: >96 %) were purchased from Tianjin Xiensopude Technology Co. Immunoglobulin M (IgM) (specification: 500 ug/ml) were purchased from Jiangsu Chentong Biotechnology Co.

2.2. P3HT OFET Preparation

In this work, a bottom-gate-top-contact structure of P3HT OFET was used (Fig. 1).

The whole device was prepared on a PET substrate covered with 65 nm thick ITO as the gate. PET/ITO was first cut into small 3 cm × 3 cm squares and fixed on a glass sheet with double sided transparent tape. Before preparing the PVA/PMMA bilayer gate media, the PET/ITO film needs to be surface cleaned in an oxygen plasma cleaner (Schwarze P3C, Beijing Jiaruntongli Technology Co., Ltd.) with oxygen pressure 600 mbar for 5 min to make the film surface hydrophilic, followed by adding 500 µl 15 mg/ml of aqueous PVA solution dropwise on the treated ITO surface, letting it cure at ambient for 12 h, and then baked in an oven at 60 °C for 120 min. Then, 500 µl 5 mg/ml

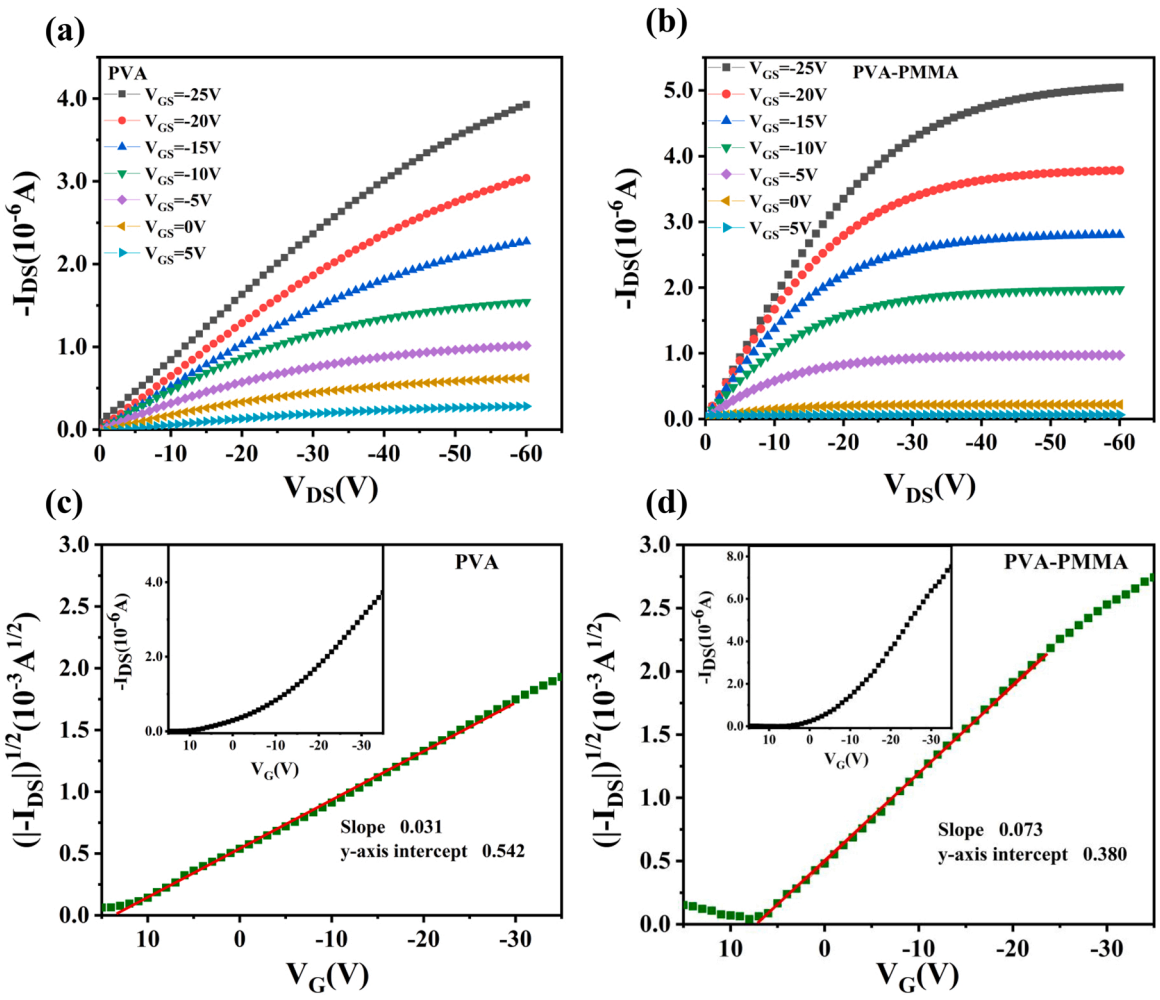

Fig. 2. Output curve (I_{DS}~V_{DS}) of (a) single PVA dielectric layer OFET and (b) double PVA-PMMA dielectric layers OFET; fitted square root current curve $\left(I_{DS}^{1/2} \sim V_G\right)$ for (c) single PVA dielectric layer OFET and (d) double PVA-PMMA dielectric layers OFET, with built-in graphs showing the transfer curve (I_{DS}~V_G) .

PMMA-anisole solution was added dropwise on PVA and annealed in an oven at 90 °C for 1 h. Finally, 100 μl of RR-P3HT-o-dichlorobenzene solution (8 mg/ml) was spin-coated on PMMA for 40 s at 2000 rpm and annealed on a hot plate at 120 °C for 10 min 3D printers were used to prepare the patterned source drain electrodes (Fan et al., 2019; Kamyshny and Magdassi, 2019; Majak et al., 2019), avoiding the disadvantages of expensive materials, time consumption and complicated lithography, vapour deposition and thermal excitation methods. The source-drain electrode pattern was set on the 3D printer with a glue output speed of 10 mm/s and channel length and width of 1.2 mm and 20 mm, respectively. Due to the fluidity of the conductive silver glue, the final channel length and width were 1.0 ± 0.2 mm and 20.5 ± 0.3 mm, respectively (width to length ratio of approximately 20). Finally, using a mask, Polydimethylsiloxane (PDMS) was deposited on the electrodes as a protective layer.

2.3. Anti-IgG deposition

Anti-IgG can be deposited on the active layer by physical adsorption for the specific detection of IgG (Fig. 1). A drop of 2 μl of anti-IgG PBS (pH = 7.4) solution, in which the antibody concentration was 100 μg/ml, was added to the exposed active layer channel. Anti-IgG was then incubated on P3HT films for 1 h, allowing sufficient immobilization of anti-IgG on the active layer, and finally, the surface of the active layer was rinsed three times with PBS standard solution to remove the excess antibody and blown dry with N_2. BSA was used as a blocking agent to prevent the nonspecific response caused by nonspecific adsorption during the assay. Three microlitres of 0.3 mg/ml BSA PBS solution was added dropwise to the functionalized active layer, incubated for 30 min, rinsed three times with PBS standard solution, and blown dry with N_2.

2.4. Characterization

The performance of an OFET can be characterized by its output and transfer characteristics. A Keithley Semiconductor Characterization Analyser (4200-SCS) was used to measure the output and transfer curves of the OFET, with the source continuously grounded under atmospheric conditions. The output curve of the OFET (I_{DS}~V_{DS}) can be measured at different gate voltages, where the gate voltage is controlled from 5 V to − 25 V in steps of − 5 V, and the drain voltage is scanned from 0 V to − 60 V, in which condition saturation region could be clearly observed. The transfer characteristic curve of the OFET (I_{DS}~V_G) is measured at a constant drain voltage. The drain voltage is set to − 30 V, and the gate voltage is scanned from 15 V to − 35 V. For the P3HT OFET, the current equation in the saturation region is as follows:

$$I_{DS} = \frac{W}{2L}\mu C_i (V_{GS}\text{-}V_{TH})^2 \quad (1)$$

In the above equation, I_{DS} is the channel current, W and L are the width and length of the channel, respectively, μ is the carrier mobility, C_i is the dielectric layer capacitance per unit area, V_G is the gate voltage,

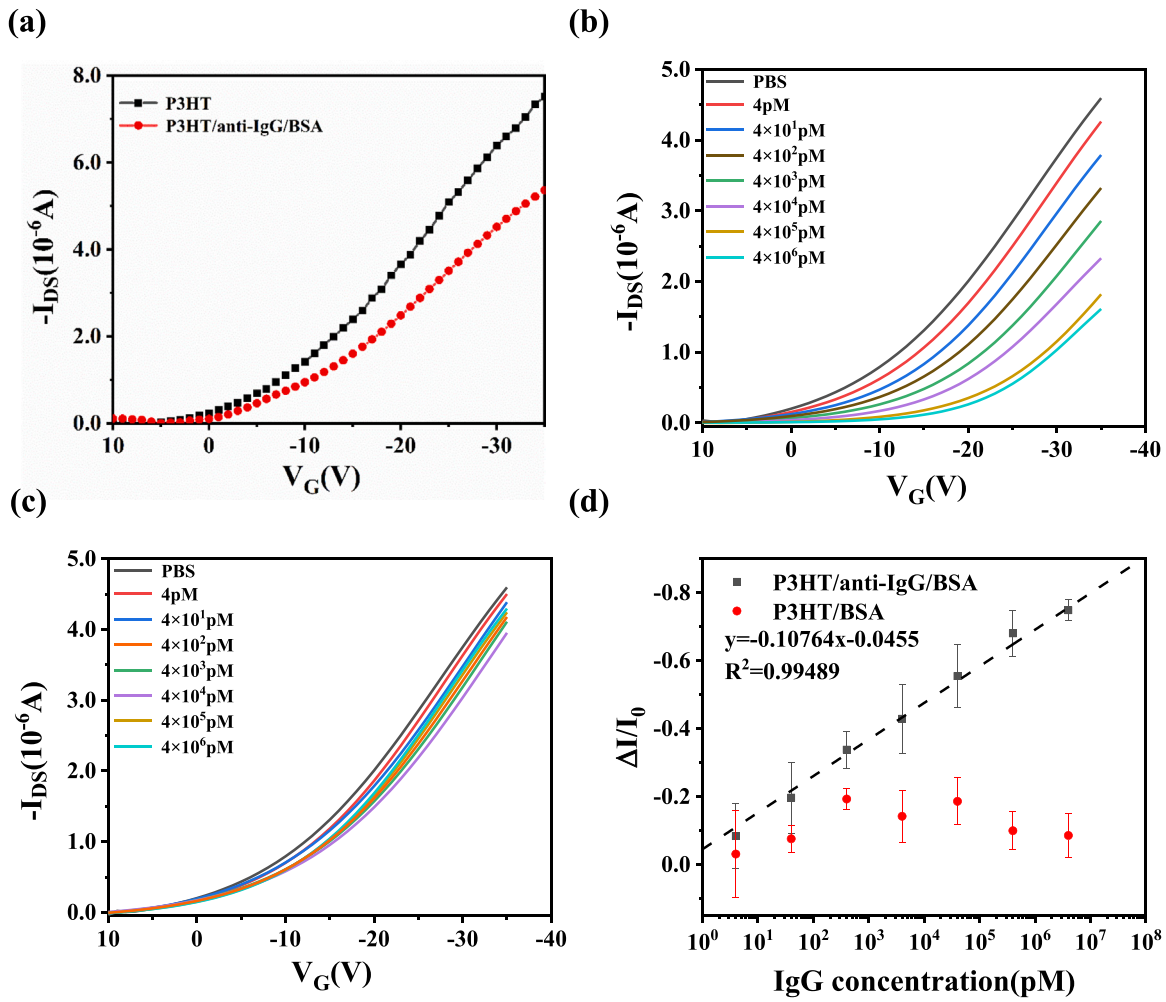

Fig. 3. (a) Transfer curve after anti-IgG/BSA modification; Transfer characteristics curves of (c) P3HT/anti-IgG/BSA and (b) P3HT/BSA P3HT-OFET when exposed to different concentrations of IgG; (d) Calibration curve obtained for the OFET (ΔI/I0 vs. log [analyte]), the line is a linear fitting of the data in semi-logarithmic scale.

V_{TH} is the threshold voltage, and V_{DS} is the drain source voltage. The saturation carrier mobility $\mu = \frac{2K^2}{(W/L)C_i}$ and the threshold voltage $V_{TH} = -\frac{A}{K}$ can be obtained from the saturation region of the transfer curve by the square extrapolation method (where K is the slope of fitted square root current curve $\left(I_{DS}^{1/2} \sim V_G\right)$ and A is its intercept on y-axis).

The specific detection of IgG by OFET can be obtained by adding different concentrations of IgG dropwise on the functionalized active layer (P3HT/anti-IgG/BSA) and measuring the current response of the transfer curves of P3HT OFET at different concentrations. The obtained transfer curves of blank measurements taken in PBS were used as the reference baseline and the source-drain current I_{DS} was taken as I_0 for $V_G = -30$ V. Subsequently, IgG concentrations of 4pM, 4×10^1pM, 4×10^2pM, 4×10^3pM, 4×10^4pM, 4×10^5pM, and 4×10^6pM PBS solutions (2 μl) were incubated on the active layer for 1 h, and then the unbound IgG was rinsed off with PBS to measure the transfer characteristic curves at different IgG concentrations. The source-drain current I_{DS} of the characteristic transfer curve at $V_G = -30$ V for different IgG concentrations was taken as I. The final current response is the ratio of the current change of the source drain current relative to the reference baseline at the same voltage when exposed to different concentrations of IgG solution (i.e., $(I-I_0)/I_0 = \Delta I/I_0$)(MacChia et al., 2019; Macchia et al., 2018). The current response induced by different concentrations (from 4 to 4×10^6 pM) of IgG was repeatedly measured on the same sensor, and the resulting current response calibration curve of the sensor was constructed. Reproducibility was assessed by comparing the relative standard deviations of the current responses obtained at identical concentrations of 5 devices. The detection limit of the P3HT OFET sensor for IgG was defined as the concentration of IgG at which the elicited response was $(\Delta I'/I_0)_{mean} + 3\sigma$, where $(\Delta I'/I_0)_{mean}$ is the average current response of the blank control, and σ is the standard deviation. Additionally, the sensor selectivity was verified by comparing the current response with that of the active layer (P3HT/BSA) not functionalized with anti-IgG. The previous procedure was repeated to study the current response of the P3HT/BSA field-effect transistor to different concentrations of IgG.

3. Results and discussion

3.1. Characterization of P3HT OFET electrical properties

OFETs with P3HT as the active layer were prepared using a bottom-gate-top-contact structure. The electrical properties of the devices were investigated by obtaining their output and transfer curves with a single layer of PVA and a double layer of PVA-PMMA as the dielectric layer. Fig. 2 shows the typical characteristic curves of the PVA single layer and PVA-PMMA double layer as the dielectric layer, where Fig. 2(a) and (b) shows the output curve, and Fig. 2(c) and (d) shows the transfer curve. Both characteristic curves show typical FET characteristics with a P-type semiconductor as the active layer where the source drain current is regulated by the gate source voltage. The P3HT OFET drain current based on a PVA-PMMA dielectric layer shows a more pronounced

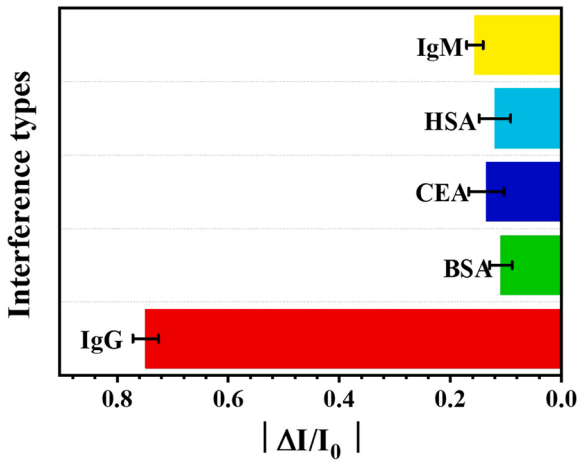

Fig. 4. Current response of the OFET sensor to other interferents.

saturation region than that of a single PVA dielectric layer (Fig. 2(a) and (b)). A linear fit of the transfer curves using the square extrapolation method (Fig. 2(c) and (d)) yields the carrier mobility μ and threshold voltage VTH for both layers. The P3HT OFET with a PVA-PMMA bilayer dielectric layer shows better electrical performance with a carrier mobility of 4.6×10^{-2} cm^2/Vs and a threshold voltage of 5.2 V, compared to the P3HT OFET with a PVA single layer dielectric layer (carrier mobility 6.3×10^{-3} cm^2/Vs, threshold voltage 17.5 V) and typical PMMA single layer (carrier mobility 0.01 cm^2/Vs, threshold voltage 44 V) (Gburek and Wagner, 2010).

The difference in the performance of the P3HT OFET based on single PVA and double PVA-PMMA dielectric layers is mainly due to the different polarities of the different dielectric layers. According to Avila et al. (2018) and Zhang et al. (2019), the water contact angle of the PVA film is 36.07° with a surface energy of 61.42 mJm^{-2}, and the water contact angle of the PMMA film is ~70.30° with a surface energy of 47.4 mJm^{-2}. The weaker polarity of the PVA-PMMA dielectric layer compared to the PVA dielectric layer helps to improve carrier transport in P3HT. In addition, the surface of the PVA film has a large number of hydrophilic hydroxyl groups, which will adsorb water molecules in the atmosphere and trap the carriers, thereby hindering carrier transport. By depositing PMMA film on PVA to form a double dielectric layer, the number of traps can be reduced, enhancing the carrier mobility of the device. Moreover, with the reduction in the number of traps, when the gate voltage is applied, no excessive gate voltage is needed to induce carriers to fill the traps, which results in a significant reduction in the threshold voltage of the P3HT OFET with a double-layer PVA-PMMA dielectric layer.

3.2. Characterization of P3HT OFET sensing performance

A study was conducted to compare the transfer curves of P3HT OFET before functionalization (pure P3HT) and after physisorption of anti-IgG receptors with BSA (Fig. 3(a)). The transfer curve of the P3HT OFET after functionalization shows a good field effect modulation current, albeit slight reduced, and the field effect mobility is comparable to that before functionalization (approximately 10^{-2} cm^2/Vs). In addition, the threshold voltage does not change significantly and remains less than 10 V.

Physisorption of anti-IgG receptors and BSA on organic semiconductor layers resulted in less pronounced changes in carrier mobility and threshold voltage of the P3HT OFET. Compared to modification by chemical reagents using covalent chemical bonds to immobilize the recognition receptors, physisorption is a gentler deposition method that does not disrupt the molecular structure of the active layer. Physisorption using intermolecular interaction forces decreases the source leakage current of the device, and the slight change in mobility may be caused by the ionic doping of the P3HT active layer, resulting in a change in carrier concentration (Mulla et al., 2015). However, the effect of this factor on the P3HT OFET is relatively small, and a slight change in carrier concentration does not cause a significant change in device performance. More importantly, label-free and selective detection of IgG can be achieved by physisorption of anti-IgG and BSA. In addition, compared to immobilizing the recognition receptor for IgG detection by chemical bonding, the process of physisorption is shorter (typically less than 2 h) and requires fewer complex operational steps.

The functionalized P3HT OFET was exposed to increasing concentrations of IgG PBS solution, and the effect of IgG binding to anti-IgG on P3HT OFET was investigated by comparing the transfer curves at different concentrations. As seen in Fig. 3(b), the drain current decreases as the IgG concentration increases (from 4 pM to 4×10^6 pM). We present a set of control experiments to validate the selective detection of IgG by our biosensor. Using the sensors not modified with anti-IgG (P3HT/BSA) exposed to increasing concentrations of IgG, Fig. 3(c) shows that the drain current of the sensors decrease with increasing IgG concentration, but the change is not significant. This proves the selectivity of the OFET towards IgG detection.

In the P3HT OFET, the specific binding of IgG and anti-IgG caused a significant change in the drain current of the device. The reason for the change in the drain current could be that the charged target molecule, when combined with the recognition element, changes the charge distribution in the active layer channel, decreasing the carrier concentration in the channel. Another possible reason is that the number of carriers that can move decreases due to the introduction of traps by the target analyte, which increases the density of trapped states and increases the probability of carrier trapping. In addition, when IgG and anti-IgG interact with each other, it is likely to change the conformation of anti-IgG and thus the conformation of the active layer itself, such as the molecular chain orientation and crystallinity of P3HT, which affects the carrier transport in the active layer channel. In conclusion, the changes in P3HT OFET-related parameters caused by the binding of IgG and anti-IgG can be seen as a shift from a small biological signal to a large electrical signal, which enables the detection of IgG.

The relative current changes induced by the dropwise addition of different concentrations of IgG PBS standard solutions on the functionalized active layer were used to characterize sensing response of the P3HT OFET. The dose curve of $\Delta I/I_0$ versus IgG concentration measured with the active layer functionalized with anti-IgG and BSA (P3HT/anti-IgG/BSA) is shown as grey scatters in Fig. 4(d), while red scatters are the negative control response measured when the active layer not functionalized with anti-IgG (P3HT/BSA) was exposed to different concentrations of IgG.

Table 1
Biosensors for detection of IgG.

Method	Analyte	Detection Range	LOD	Label
OFET (This work)	IgG	4 pM-4 × 10^6pM	2.9pM	Label free
EGOFET (Macchia et al., 2018)	IgG	6zM-6 × 10^6pM	1 ± 1 Protein	Label free
Extend-Gate OFET (Minamiki et al., 2014)	IgG	0 pM – 6.5 × 10^4pM	4 nM	Label free
QCM (Zhou et al., 2021)	IgG	–	7pM	Label free
Fluorescent Immunoassays (Spindel et al., 2015)	IgG	–	175pM	Label needing

As shown in Fig. 4(d), the current response of the unfunctionalized P3HT OFET to IgG did not changed significantly with increasing IgG concentration. In contrast, the current response of the functionalized P3HT OFET varies almost linearly with increasing IgG concentration and ranges across 6 orders of magnitude (from 4 pM to 4×10^6 pM), reflecting the selective detection of IgG by the functionalized P3HT OFET. In addition, the current response was 2.9 pM when the current response was $(\Delta I^{'}/I_0)_{mean} + 3\sigma = 0.0957$, where $(\Delta I^{'}/I_0)_{mean}$ is the average value of the blank response and σ is its standard deviation. So the LOD of our sensor is 2.9 pM and the LOQ is 4.3 pM using the same calculation method. The relative standard deviation of individual calibration points on the current response curves tested on five different functionalized P3HT OFET chips was less than 11 %, indicating good reproducibility between devices for IgG detection.

In order to evaluate the selectivity of the sensor, the prepared sensor was used to conduct an interference comparison test for 4×10^6 pM of other interfering analytes such as IgM, HSA, CEA and BSA, as shown in Fig. 4. The sensor exhibited a higher change in current response to the same concentration of IgG than to other interfering analytes. It can be seen that the sensor has good selectivity for IgG detection.

Table 1 is a comparison of this work and other works related to IgG detection. Traditional fluorescent immunoassays require fluorescent labeling of proteins, which may damage them. Quartz crystal microbalance (QCM) sensors do not need label, but the operation is cumbersome. Field-effect transistor-based biosensors not only require no labels, but also have relatively low detection limits. However, EGOFET biosensors require chemical bonds to immobilize recognition elements, which may disrupt the structure of biomolecules. Therefore, this work not only have a simplified preparation process, but also uses physical adsorption to immobilize the antibody, and realizes the label-free detection of IgG, which is helpful for the further development of field effect transistor biosensors.

4. Conclusion

A double-layer dielectric layer-based P3HT OFET was developed for label-free detection of IgG by combining a 3D printed source drain electrode with an active layer for direct physisorption of anti-IgG. The results show that the P3HT OFET with a double-layer dielectric layer outperforms the single-layer dielectric layer and enables label-free detection of target analytes down to pM by direct physisorption of the identified elements. The preparation of the P3HT OFET biosensor proposed in this paper is not only easy to operate but also uses inexpensive materials, which has profound implications for the further commercialization of the P3HT OFET biosensor. Compared with other analytical methods, this sensor has the advantages of a wide detection range, low detection limit, and high selectivity, providing guidance for the development of a new generation of OFET biosensors.

CRediT authorship contribution statement

Hao Runfang: Supervision. **Yue Yangfan:** Investigation, Writing – original draft. **Li Leilei:** Validation, **Ji Jianlong:** Project administration. **Zhang Qiang:** Project administration. **Ding Lifeng:** Writing – review & editing. **Sang Shengbo:** Supervision. **Li Qiang:** Conceptualization, Methodology, Writing – review & editing, Funding acquisition.

Declaration of Competing Interest

The authors declare the following financial interests/personal relationships which may be considered as potential competing interests: Qiang Li reports financial support was provided by Science and Technology Department of Shanxi Province.

Data Availability

Data will be made available on request.

Acknowledgements

This research was funded by the Applied Basic Research Programs of Science and Technology Department of Shanxi Province, grant number 20210302124197 and 20210302123136, and the Scientific and Technological Innovation Programs of Higher Education Institutions in Shanxi, grant number 2019L0235 and 2021L535.

References

Albers, W.M., Pelto, J.M., Suspène, C., Määttä, J.A., Yassar, A., Hytönen, V.P., Vikholm-Lundin, I.M., Tappura, K., 2012. Structural and functional characteristics of chimeric avidins physically adsorbed onto functionalized polythiophene thin films. ACS Appl. Mater. Interfaces 4, 4067–4077.

Avila, H.C., Serrano, P., Barreto, A.R.J., Ahmed, Z., Gouvêa, C., de, P., Vilani, C., Capaz, R.B., Marchiori, C.F.N., Cremona, M., 2018. High hole-mobility of rrP3HT in organic field-effect transistors using low-polarity polyurethane gate dielectric. Org. Electron. 58, 33–37.

Awsiuk, K., Budkowski, A., Petrou, P., Marzec, M.M., Biernat, M., Jaworska-Gołąb, T., Rysz, J., 2016. Orientation and biorecognition of immunoglobulin adsorbed on spin-cast poly(3-alkylthiophenes): impact of polymer film crystallinity. Colloids Surf. B Biointerfaces 148, 278–286.

Awsiuk K., Budkowski A., Marzec M.M., Petrou P., Rysz J. and Bernasik A., 2014 Effects of polythiophene surface structure on adsorption and conformation of bovine serum albumin: A mul1. K. Awsiuk, A. Budkowski, M. M. Marzec, P. Petrou, J. Rysz and A. Bernasik, Langmuir, 30, 13925 (2014).tivariate and multitechnique study Langmuir 30 13925–13933.

Cao, X., Li, H., Li, G., Gao, X., 2019. Electrocatalytically active MoSe2 counter electrode prepared in situ by magnetron sputtering for a dye-sensitized solar cell. Chin. J. Catal. 40, 1360–1365.

Casalini, S., Leonardi, F., Cramer, T., Biscarini, F., 2013. Organic field-effect transistor for label-free dopamine sensing. Org. Electron. 14, 156–163.

Di, Y., Yaofeng, Z., 2021. The characters and applications of livestock immunoglobulins. Chem. life 41, 1154–1159.

Fan, J., Montemagno, C., Gupta, M., 2019. 3D printed high transconductance organic electrochemical transistors on flexible substrates. Org. Electron. 73, 122–129.

Ferhati, H., Djeffal, F., Benhaya, A., 2019. Optimized high-performance ITO/Ag/ITO multilayer transparent electrode deposited by RF magnetron sputtering. Superlattices Microstruct. 129, 176–184.

Frisk, G., Torfason, E.G., Diderholm, H., 1984. Reverse radioimmunoassays of IgM and IgG antibodies to coxsackie B viruses in patients with acute myopericarditis. J. Med. Virol. 14, 191–200.

Gburek, B., Wagner, V., 2010. Influence of the semiconductor thickness on the charge carrier mobility in P3HT organic field-effect transistors in top-gate architecture on flexible substrates. Org. Electron. 11, 814–819.

Hammock, M.L., Knopfmacher, O., Naab, B.D., Tok, J.B.H., Bao, Z., 2013. Investigation of protein detection parameters using nanofunctionalized organic field-effect transistors. ACS Nano 7, 3970–3980.

Huynh, T.M., Nguyen, T.S.V., Doan, T.C.D., Dang, C.M., 2019. Fabrication of thin film Ag/AgCl reference electrode by electron beam evaporation method for potential measurements. Adv. Nat. Sci. Nanosci. Nanotechnol. 10, 0–6.

Janmanee, R., Baba, A., Phanichphant, S., Sriwichai, S., Shinbo, K., Kato, K., Kaneko, F., 2011. Detection of human IgG on Poly(pyrrole-3-carboxylic acid) thin film by electrochemical-Surface plasmon resonance spectroscopy. Jpn. J. Appl. Phys. 50, 1–6.

Jiajun, T., Pinhe, H., Qianlan, Y., Qili, H., 2020. Establishment of immunosuppressive animal models in mice and their rapid detection. Chin. J. Comp. Med. 30, 11–82.

Jian, J., 2021. Effects of cyclophosphamide combined with prednisone on inflammatory factors, lymphocyte subsets and immune function in patients with systemic lupus erythematosus. Contemp. Med. 27, 62–64.

Kamyshny, A., Magdassi, S., 2019. Conductive nanomaterials for 2D and 3D printed flexible electronics. Chem. Soc. Rev. 48, 1712–1740.

Kikuti, M., Tauro, L.B., Moreira, P.S.S., Campos, G.S., Paploski, I.A.D., Weaver, S.C., Reis, M.G., Kitron, U., Ribeiro, G.S., 2018. Diagnostic performance of commercial IgM and IgG enzyme-linked immunoassays (ELISAs) for diagnosis of Zika virus infection. Virol. J. 15, 1–7.

Kim, Y.S., Yoo, T.K., Chung, C.H., 2020. Microchip sensor of PdO-NiO electrode for H2O2 sensing fabricated with the UV photolithography. Korean J. Chem. Eng. 37, 1810–1820.

Lanxia, Q., 2018. Study on immunoglobulin IgG in bovine colostrum powder enhanced immune function. Mod. Food 111–115.

Lin, P., Yan, F., 2012. Organic thin-film transistors for chemical and biological sensing. Adv. Mater. 24, 34–51.

Macchia, E., Manoli, K., Holzer, B., Di Franco, C., Ghittorelli, M., Torricelli, F., Alberga, D., Mangiatordi, G.F., Palazzo, G., Scamarcio, G., Torsi, L., 2018. Single-molecule detection with a millimetre-sized transistor. Nat. Commun. 9, 3223.

Macchia, E., Manoli, K., Holzer, B., Franco, C.D., Ghittorelli, M., Torricelli, F., Alberga, D., Mangiatordi, G.F., Palazzo, G., Scamarcio, G., Torsi, L., 2018. Single-molecule detection with a millimetre-sized transistor. Nat. Commun. 9, 3223.
MacChia, E., Tiwari, A., Manoli, K., Holzer, B., Ditaranto, N., Picca, R.A., Cioffi, N., Di Franco, C., Scamarcio, G., Palazzo, G., Torsi, L., 2019. Label-free and selective single-molecule bioelectronic sensing with a millimeter-wide self-assembled monolayer of anti-immunoglobulins. Chem. Mater. 31, 6476–6483.
Magliulo, M., Mallardi, A., Gristina, R., Ridi, F., Sabbatini, L., Cioffi, N., Palazzo, G., Torsi, L., 2013. Part per trillion label-free electronic bioanalytical detection. Anal. Chem. 85, 3849–3857.
Magliulo, M., De Tullio, D., Vikholm-Lundin, I., Albers, W.M., Munter, T., Manoli, K., Palazzo, G., Torsi, L., 2016. Label-free C-reactive protein electronic detection with an electrolyte-gated organic field-effect transistor-based immunosensor. Anal. Bioanal. Chem. 408, 3943–3952.
Majak, D., Fan, J., Gupta, M., 2019. Fully 3D printed OECT based logic gate for detection of cation type and concentration. Sens. Actuators B Chem. 286, 111–118.
Minamiki, T., Minami, T., Kurita, R., Niwa, O., Wakida, S.I., Fukuda, K., Kumaki, D., Tokito, S., 2014. A label-free immunosensor for IgG based on an extended-gate type organic field effect transistor. Materials 6, 6843–6852.
Mizutani, N., Korposh, S., Selyanchyn, R., Wakamatsu, S., Lee, S.W., 2012. Application of a quartz crystal microbalance (QCM) twin sensor for selective label-free immunoassay to simultaneous antigen-antibody reactions. Sens. Transducers 137, 1–9.
Mulla, M.Y., Seshadri, P., Torsi, L., Manoli, K., Mallardi, A., Ditaranto, N., Santacroce, M. V., Franco, C.D., 2015. Scamarcioc G and Magliulo M. UV crosslinked poly(acrylic acid): a simple method to bio-functionalize electrolyte-gated OFET biosensors. J. Mater. Chem. B 3, 5049–5057.
Pas, S.D., Streefkerk, R.H.R.A., Pronk, M., de Man, R.A., Beersma, M.F., Osterhaus, A.D. M.E., Van der Eijk, A.A., 2013. Diagnostic performance of selected commercial HEV IgM and IgG ELISAs for immunocompromised and immunocompetent patients. J. Clin. Virol. 58, 629–634.
Qian, qian J., Bin, L., 2021. Relationship between expression of immunoglobulin and complement and disease activity in patients with systemic lupus erythematosus. Chin. J. Sch. Dr. 35, 789–791.
Sailapu, S.K., Macchia, E., Merino-Jimenez, I., Esquivel, J.P., Sarcina, L., Scamarcio, G., Minteer, S.D., Torsi, L., Sabaté, N., 2020. Standalone operation of an EGOFET for ultra-sensitive detection of HIV. Biosens. Bioelectron. 156, 112103–1.
Santos, L., da, S., Fernandes, V.C., da Cruz, S.G., Siqueira, W.C., Goes, A.M., Pedroso, Ê.R. P., 2012. Profile of total Igg, Igg1, Igg2, Igg3 and Igg4 levels in sera of patients with paracoccidioidomycosis: Treatment follow-up using Mexo and rPb27 as antigens in an ELISA. Mem. Inst. Oswaldo Cruz 107, 1–10.
Seshadri, P., Manoli, K., Schneiderhan-Marra, N., Anthes, U., Wierzchowiec, P., Bonrad, K., Di Franco, C., Torsi, L., 2018. Low-picomolar, label-free procalcitonin analytical detection with an electrolyte-gated organic field-effect transistor based electronic immunosensor. Biosens. Bioelectron. 104, 113–119.
Shi, J., Yao, Y., Xue, L., Li, K., Ning, J., Jiang, F., Huang, F., 2020. Application of magnetron sputtering to deposit a multicomponent separator with polysulfide chemisorption and electrode stabilization for high-performance lithium-sulfur batteries. Surf. Coat. Technol. 405, 126580.
Shikun, H., 2022. Correlations among serum immunoglobulin levels and disease activity in patients with systemic lupus erythematosus. Med. J. Chin. People's Heal 34, 112–114.
Spindel, S., Balsam, J., Mattay, G., Sapsford, K.E., 2015. Investigating low volume planar surface fluorescent immunoassays with QDs for spatial and spectral multiplexing. Sens. Actuators B Chem. 215, 396–404.
Sun, H.T., Wang, X.P., Kou, Z.Q., Wang, L.J., Wang, J.Y., Sun, Y.Q., 2015. Optimization of TiO2/Cu/TiO2 multilayers as a transparent composite electrode deposited by electron-beam evaporation at room temperature. Chin. Phys. B 24.
Syu, Y.-C., Hsu, W.-E., Lin, C.-T., 2018. Review—field-effect transistor biosensing: devices and clinical applications. ECS J. Solid State Sci. Technol. 7, 3196–3207.
Vasilyeva, M.S., Rudnev, V.S., Zykova, E.S., Ustinov, A.Y., Sergeeva, K.A., Nepomnyaschiy, A.V., Lukiyanchuk, I.V., Marinina, G.I., 2018. FtI/TiO2,Au electrodes prepared by plasma electrolytic oxidation and electron beam evaporation *Defect Diffus*. Forum 386, 326–331.
Wang, N., Yang, A., Fu, Y., Li, Y., Yan, F., 2019. Functionalized organic thin film transistors for biosensing. Acc. Chem. Res. 52, 277–287.
Wu, Q., Song, D., Zhang, D., Sun, Y., 2016. An enhanced SPR immunosensing platform for human IgG based on the use of silver nanocubes and carboxy-functionalized graphene oxide. Microchim. Acta 183, 2177–2184.
Xue, F., Liu, Z., Su, Y., Varahramyan, K., 2005. Inkjet printed silver source/drain electrodes for low-cost polymer thin film transistors. Microelectron. Eng. 83, 298–302.
Zhang, H., Zhang, F., Sun, J., Zhang, M., Hu, Y., Lou, Z., Hou, Y., 2019. Applied Surface Science Solution-processed organic field-e ff ect transistors with cross-linked poly (4-vinylphenol)/ polyvinyl alcohol bilayer dielectrics. Appl. Surf. Sci. 478, 699–707.
Zhou, L., Kato, F., Ogi, H., 2021. Sensitive label-free IgG detection using MEMS QCM biosensor with 125-MHz wireless quartz resonator. Jpn. J. Appl. Phys. 60, 1–4.